THE CRACK PROBLEM IN A REINFORCED

CYLINDRICAL SHELL

O. Selcuk Yahsi and F. Erdogan

March 1986

Lehigh University
Bethlehem, Pennsylvania

THE CRACK PROBLEM IN A REINFORCED
CYLINDRICAL SHELL*

by

O. Selcuk Yahsi** and F. Erdogan
Lehigh University, Bethlehem, PA 18015

ABSTRACT

In this paper a partially reinforced cylinder containing an axial through crack is considered. The reinforcement is assumed to be fully bonded to the main cylinder. The composite cylinder is thus modelled by a nonhomogeneous shell having a step change in the elastic properties at the z=0 plane, z being the axial coordinate. Using a Reissner type transverse shear theory the problem is reduced to a pair of singular integral equations. In the special case of a crack tip touching the bimaterial interface it is shown that the dominant parts of the kernels of the integral equations associated with both membrane loading and bending of the shell reduce to the generalized Cauchy kernel obtained for the corresponding plane stress case. The integral equations are solved and the stress intensity factors are given for various crack and shell dimensions. A bonded fiberglass reinforcement which may serve as a crack arrestor is used as an example.

1. Introduction

In studying the failure of structures for the purpose of calculating the fracture mechanics parameters, a very large variety of structural components may locally be modelled as relatively thin-walled plates or shells. Nearly all "pressure boundaries" and piping as well as some important parts of aerospace and hydrospace structures may be cited as examples of such components. From a viewpoint of structural integrity two of the important questions one may be concerned with in this respect are the life estimate based on the subcritical growth of an existing flaw and the residual strength or the load carrying capacity of the structure based on the criticality of a dominant flaw. In most cases the two questions may be adequately dealt with by idealizing the component with a plate or a shell and the flaw with a

---

(**) Permanent address: Department of Mechanical Engineering, Middle East Technical University, Ankara, Turkey.

part-through or a through crack, by calculating the appropriate fracture mechanics parameter (e.g., the stress intensity factor), and by applying a suitable criterion along with the baseline characterization of the material.

In relatively thin-walled structures the inherently three-dimensional crack problem is approximated by a "plate" or a "shell" problem, that is, by suppressing the thickness coordinate through the use of a plate or a shell theory. In the earlier studies of the subject the classical plate and shell theories were used to solve the problem (see, for example, [1] for review). However, particularly in problems requiring the calculation of the stress intensity factors, the necessity of using a higher order theory has now been well-established. For example, it has been shown that by using a Reissner type transverse shear theory [2] (and hence by satisfying the boundary conditions on the crack surfaces for all stress and moment resultants separately) one could obtain an asymptotic stress state around the crack tips which is identical to that given by the in-plane and anti-plane elasticity solutions (see, for example, [3], [4] and [5]). Furthermore, it has also been shown that in the limiting case of small crack lengths these plate and shell results approach that of plane elasticity not only for the internal but also for the edge cracks [6], [7], [8]. Other results obtained by using a transverse shear theory for various crack-shell geometries and loading conditions may be found in [9]-[12].

With the exception of [7], [8] and [13], in all crack studies in shells that appeared in literature the shell is assumed to be "infinite" in the sense that the interaction of the perturbation field of the crack with the boundaries of or with other geometric discontinuities in the shell are assumed to be negligible. The interaction of the stress field around the crack with a stress-free boundary and with a fully clamped boundary in a cylindrical shell was considered in [7] and [8], respectively, where the special case of the crack intersecting the boundary has also been studied. In [13] the interaction of a crack field with a circumferential line stiffener in a cylindrical shell was studied by using the classical shell theory. In this paper we consider the somewhat more general problem of a nonhomogeneous cylindrical shell containing an axial crack. The problem studied is that of two relatively long cylinders having the same radii and different mechanical properties that are joined along their boundaries at a plane perpendicular to their

common axis (Fig. 1b). The model may be used to simulate composite cylinders, cylinders with reinforcing layers, and homogeneous cylinders having a step change in thickness (Fig. 1a and b). Such solutions are needed or may be very useful in, for example, crack arrest studies in pipes and containers with reinforcements.

2. General Formulation of the Problem

The analytical problem under consideration is described in Fig. 1b. The actual problem may arise, for example, from a reinforced shell shown in Fig. 1a. Since "shell theory" is used in formulating the problem, whatever the actual configuration and composition of the medium for $x_2 > 0$, it has to be reduced to a homogeneous shell having the same radii as the semi-infinite cylinder occupying $x_2 < 0$. The first step in the solution of the problem is, therefore, the determination of the elastic properties E_2, ν_2 of an ("infinitely" long) equivalent shell of thickness h in terms of E_1, ν_1, E', ν', h, h_2 and R_i where E' and ν' may or may not be the same as E_1 and ν_1. This step is briefly described in Appendix B where the composite cylinder is assumed to consist of fully-bonded thick-walled cylinders under axisymmetric plane strain condition and the equivalency of the radial displacements and axial strains is used to determine E_2 and ν_2.

Details of the formulation of a homogeneous shallow shell containing a through crack by using a Reissner type transverse shear theory may be found, for example, in [9]-[11] and will not be repeated here. Thus, referring to Appendix A for the definition of normalized and dimensionless quantities, in terms of the displacement w, stress function ϕ and the auxiliary functions ψ and Ω, the basic equations for the nonhomogeneous cylindrical shell shown in Fig. 1b may be expressed as follows:

$$\nabla^4\phi - (\lambda_i/\mu_i)^2 \frac{\partial^2 w}{\partial y^2} = 0 \ , \ (i=1, \ y<0; \ i=2, \ y>0) \tag{1}$$

$$\nabla^4 w + \lambda_i^2\mu_i^2(1-\kappa_i\nabla^2) \frac{\partial^2\phi}{\partial y^2} = 0, \ (i=1, \ y<0; \ i=2, \ y>0) \ , \tag{2}$$

$$\kappa_i\nabla^2\psi - \psi - w = 0, \ (i=1, \ y<0; \ i=2, \ y>0) \ , \tag{3}$$

$$\frac{\kappa_i(1-\nu_i)}{2} \nabla^2\Omega - \Omega = 0, \ (i=1, \ y<0; \ i=2, \ y>0) \tag{4}$$

-3-

where the constants λ_i, μ_i and κ_i (i=1,2) are defined in Appendix A, ν_i is the Poisson's ratio, it is assumed that the cylindrical surfaces of the composite shell are free of tractions and the crack surface stress and moment resultants are the only nonzero external loads. The functions ψ and Ω are related to the rotations as follows:

$$\beta_x = \frac{\partial \psi}{\partial x} + \frac{\kappa_i(1-\nu_i)}{2} \frac{\partial \Omega}{\partial y} , \quad \beta_y = \frac{\partial \psi}{\partial y} - \frac{\kappa_i(1-\nu_i)}{2} \frac{\partial \Omega}{\partial x} ,$$

$$(i=1, y<0; i=2, y>0) . \qquad (5)$$

The normalized membrane, moment and transverse shear resultants are given by

$$N_{xx} = \frac{\partial^2 \phi}{\partial y^2} , \quad N_{yy} = \frac{\partial^2 \phi}{\partial x^2} , \quad N_{xy} = -\frac{\partial^2 \phi}{\partial x \partial y} , \qquad (6)$$

$$M_{xx} = \frac{a}{h\mu_i^4} (\frac{\partial \beta_x}{\partial x} + \nu_i \frac{\partial \beta_y}{\partial y}) , \quad M_{yy} = \frac{a}{h\mu_i^4} (\nu_i \frac{\partial \beta_x}{\partial x} + \frac{\partial \beta_y}{\partial y}) ,$$

$$M_{xy} = \frac{a}{h\mu_i^4} \frac{1-\nu_i}{2} (\frac{\partial \beta_x}{\partial y} + \frac{\partial \beta_y}{\partial x}) , \quad (i=1, y<0; i=2, y>0) , \qquad (7)$$

$$V_x = \frac{\partial w}{\partial x} + \beta_x , \quad V_y = \frac{\partial w}{\partial y} + \beta_y . \qquad (8)$$

Eliminating ϕ, from (1) and (2) it may be shown that

$$\nabla^4 \nabla^4 w + \lambda_i^4 (1-\kappa_i \nabla^2) \frac{\partial^2 w}{\partial y^2} = 0 , \quad (i=1, y<0; i=2, y>0) . \qquad (9)$$

If we express the solution of (9) by

$$w(x,y) = \begin{cases} \frac{1}{2\pi} \int_{-\infty}^{\infty} f_1(x,\alpha)e^{-i\alpha y}d\alpha + \frac{2}{\pi} \int_{0}^{\infty} f_2(y,\beta)\cos\beta x d\beta , \quad (y<0) , \\ \\ \frac{2}{\pi} \int_{0}^{\infty} f_3(y,\beta)\cos\beta x d\beta , \quad (y>0) , \end{cases} \qquad (10)$$

and assume the solution of the ordinary differential equations resulting from (9) and (10) of the form

$$f_1(x,\alpha) = R_1(\alpha)e^{m_1 x} \quad , \quad f_2(y,\beta) = R_2(\beta)e^{m_2 y} \quad ,$$

$$f_3(y,\beta) = R_3(\beta)e^{m_3 y} \quad , \tag{11}$$

The characteristic equations giving m_1, m_2 and m_3 may be obtained as follows:

$$m_1^8 - 4\alpha^2 m_1^6 + 6\alpha^4 m_1^4 - (4\alpha^2 + \kappa_1 \lambda_1^4)\alpha^4 m_1^2 + \alpha^4[\alpha^4 + \lambda_1^4(1 + \kappa_1 \alpha^2)] = 0 \quad , \tag{12}$$

$$m_2^8 - (4\beta^2 + \kappa_1 \lambda_1^4)m_2^6 + (6\beta^4 + \kappa_1 \lambda_1^4 \beta^2 + \lambda_1^4)m_2^4 - 4\beta^6 m_2^2 + \beta^8 = 0 \quad , \tag{13}$$

$$m_3^8 - (4\beta^2 + \kappa_2 \lambda_2^4)m_3^6 + (6\beta^4 + \kappa_2 \lambda_2^4 \beta^2 + \lambda_2^2)m_3^4 - 4\beta^6 m_3^2 + \beta^8 = 0 \quad . \tag{14}$$

We designate the roots of (12)-(14) by m_{ij}, $i=1,2,3$, $j=1,...,8$ and note that, properly ordered, they have the following properties:

$$\text{Re}(m_{ij}) < 0, \quad m_{ij+4} = -m_{ij} \quad , \quad (i=1,2,3, \ j=1,2,3,4) \quad . \tag{15}$$

Assuming that the composite shell shown in Fig. 1b is loaded symmetrically, it is sufficient to consider the problem for $x>0$ only. Also, since the external loads acting on the crack surfaces are statically self-equilibrating, the functions f_1, f_2 and f_3 must vanish at infinity and may, therefore be expressed as

$$f_1(x,\alpha) = \sum_{j=1}^{4} R_{1j}(\alpha)e^{m_{1j} x} \quad , \quad x>0 \quad , \tag{16}$$

$$f_2(y,\beta) = \sum_{j=5}^{8} R_{2j}(\beta)e^{m_{2j} y} \quad , \quad y<0 \quad , \tag{17}$$

$$f_3(y,\beta) = \sum_{j=1}^{4} R_{3j}(\beta)e^{m_{3j} y} \quad , \quad y>0 \quad , \tag{18}$$

Similarly, if we let

$$\phi(x,y) = \begin{cases} \dfrac{1}{2\pi}\displaystyle\int_{-\infty}^{\infty} g_1(x,\alpha)e^{-i\alpha y}d\alpha + \dfrac{2}{\pi}\displaystyle\int_0^{\infty} g_2(y,\beta)\cos\beta x\,d\beta, & (y<0) \\[2ex] \dfrac{2}{\pi}\displaystyle\int_0^{\infty} g_3(y,\beta)\cos\beta x\,d\beta, & (y>0), \end{cases} \tag{19}$$

from (1), (2), (10) and (16)-(18) it may be shown that [10]

$$g_1(x,\alpha) = -\frac{\lambda_1^2}{\mu_1^2}\alpha^2 \sum_{j=1}^{4} \frac{R_{1j}(\alpha)}{p_{1j}^2} e^{m_{1j}x}, \quad (x>0), \tag{20}$$

$$g_2(y,\beta) = \frac{\lambda_1^2}{\mu_1^2} \sum_{j=5}^{8} \frac{m_{2j}^2 R_{2j}(\beta)}{p_{2j}^2} e^{m_{2j}y}, \quad (y<0), \tag{21}$$

$$g_3(y,\beta) = \frac{\lambda_2^2}{\mu_2^2} \sum_{j=1}^{4} \frac{m_{3j}^2 R_{3j}(\beta)}{p_{3j}^2} e^{m_{3j}y}, \quad (y>0), \tag{22}$$

where

$$p_{1j}^2 = m_{1j}^2 - \alpha^2, \quad p_{2j}^2 = m_{2j}^2 - \beta^2, \quad p_{3j}^2 = m_{3j}^2 - \beta^2. \tag{23}$$

Assuming now the solution of (3) and (4) of the form

$$\Omega(x,y) = \begin{cases} \dfrac{1}{2\pi}\displaystyle\int_{-\infty}^{\infty} h_1(x,\alpha)e^{-i\alpha y}d\alpha + \dfrac{2}{\pi}\displaystyle\int_0^{\infty} h_2(y,\beta)\sin\beta x\,d\beta, & (y<0), \\[2ex] \dfrac{2}{\pi}\displaystyle\int_0^{\infty} h_3(y,\beta)\sin\beta x\,d\beta, & (y>0) \end{cases} \tag{24}$$

$$\psi(x,y) = \begin{cases} \dfrac{1}{2\pi}\displaystyle\int_0^{\infty} k_1(x,\alpha)e^{-i\alpha y}d\alpha + \dfrac{2}{\pi}\displaystyle\int_0^{\infty} k_2(y,\beta)\cos\beta x\,d\beta, & (y<0), \\[2ex] \dfrac{2}{\pi}\displaystyle\int_0^{\infty} k_3(y,\beta)\cos\beta x\,d\beta, & (y>0) \end{cases} \tag{25}$$

It can be shown that

-6-

$$h_1(x,\alpha) = A_1(\alpha)e^{r_1 x}, \quad r_1 = -[\alpha^2 + \frac{2}{\kappa_1(1-\nu_1)}]^{\frac{1}{2}}, \quad (x>0), \tag{26}$$

$$h_2(y,\beta) = A_2(\beta)e^{r_2 y}, \quad r_2 = [\beta^2 + \frac{2}{\kappa_1(1-\nu_1)}]^{\frac{1}{2}}, \quad (y<0), \tag{27}$$

$$h_3(y,\beta) = A_3(\beta)e^{r_3 y}, \quad r_3 = -[\beta^2 + \frac{2}{\kappa_2(1-\nu_2)}]^{\frac{1}{2}}, \quad (y>0), \tag{28}$$

$$k_1(x,\alpha) = \sum_{j=1}^{4} \frac{R_{1j}(\alpha)}{\kappa_1 p_{1j}-1} e^{m_{1j}x}, \quad (x>0), \tag{29}$$

$$k_2(y,\beta) = \sum_{j=5}^{8} \frac{R_{2j}(\beta)}{\kappa_1 p_{2j}-1} e^{m_{2j}y}, \quad (y<0), \tag{30}$$

$$k_3(y,\beta) = \sum_{j=1}^{4} \frac{R_{3j}(\beta)}{\kappa_2 p_{3j}-1} e^{m_{3j}y}, \quad (y>0). \tag{31}$$

The preceding formulation contains fifteen unknown functions R_{1j}, $(j=1,\ldots,4)$, R_{2j}, $(j=5,\ldots,8)$, R_{3j}, $(j=1,\ldots,4)$, and A_i, $(i=1,2,3)$, which are determined from the following boundary and continuity conditions (see Fig. 1b and Appendix A):

$$u(x,-0)=u(x,+0), \quad v(x,-0)=v(x,+0), \quad w(x,-0)=w(x,+0), \quad (x\geq0), \tag{32}$$

$$\beta_x(x,-0)=\beta_x(x,+0), \quad \beta_y(x,-0)=\beta_y(x,+0), \quad (x\geq0), \tag{33}$$

$$E_1 N_{yy}(x,-0)=E_2 N_{yy}(x,+0), \quad E_1 N_{xy}(x,-0)=E_2 N_{xy}(x,+0), \quad (x\geq0), \tag{34}$$

$$E_1 M_{yy}(x,-0)=E_2 M_{yy}(x,+0), \quad E_1 M_{xy}(x,-0)=E_2 M_{xy}(x,+0), \quad (x\geq0), \tag{35}$$

$$B_1 V_y(x,-0) = B_2 V_y(x,+0), \tag{36}$$

$$N_{xy}(0,y)=0, \quad M_{xy}(0,y)=0, \quad V_x(0,y)=0, \quad (y<0), \tag{37}$$

$$N_{xx}(0,y) = F_1(y), \quad (-d_1<y<-b_1),$$

$$u(0,y) = 0, \quad (-\infty<y<-d_1, \quad -b_1<y<0), \tag{38a,b}$$

$$M_{xx}(0,y) = F_2(y), \quad (-d_1 < y < -b_1) \ ,$$

$$\beta_x(0,y) = 0, \quad (-\infty < y < -d_1, \ -b_1 < y < 0) \ , \tag{39a,b}$$

where F_1 and F_2 are the crack surface tractions obtained from the solution of the uncracked shell under the given external loads. Note that for $y > 0$ the assumed solution has the proper symmetry and gives

$$N_{xy}(0,y) = M_{xy}(0,y) = V_x(0,y) = \beta_x(0,y) = u(0,y) = 0 \ , \quad (y \geq 0) \ . \tag{40}$$

It is seen that once the functions w, ϕ, ψ and Ω are determined, β_i, N_{ij}, M_{ij} and V_i, $(i,j=x,y)$ may be expressed in terms of R_{ij} and A_i by using (5)-(8). To complete the formulation of the problem the displacements u and v need to be determined. This may be done by using the Hooke's law and the following kinematic relations

$$\epsilon_{ij} = \frac{1}{2} (u_{i,j} + u_{j,i} + Z_{,i}u_{3,j} + Z_{,j}u_{3,i}) \ , \quad (i,j=1,2) \ , \tag{41}$$

where the function $Z(x_1,x_2)$ describes the middle surface of the shell. For the cylindrical shell under consideration $Z_{,2} = 0$, $Z_{,11} = -1/R$ and referring to Appendix A we find

$$\frac{\partial^2 u}{\partial y^2} = 2(1+\nu_i) \frac{\partial N_{xy}}{\partial y} - \frac{\partial N_{yy}}{\partial x} + \nu_i \frac{\partial N_{xx}}{\partial x} + \frac{\lambda_i^2}{\mu_i^2} \frac{\partial^2 w}{\partial y^2} x \ , \tag{42}$$

$$\frac{\partial v}{\partial y} = N_{yy} - \nu_i N_{xx} \ , \tag{43}$$

where $i=1$ for $y<0$ and $i=2$ for $y>0$. From (42), (43) and the formulation given in this section it can be shown that

$$u(x,y) = \frac{1}{2} \frac{\lambda_1^2}{\mu_1^2} \int_{-\infty}^{\infty} \sum_{j=1}^{4} \frac{(2+\nu_1)\alpha^2 - m_{1j}^2}{p_{1j}^2} R_{1j}(\alpha) m_{1j} e^{m_{1j}x - i\alpha y} d\alpha$$

$$+ \frac{2}{\pi} \frac{\lambda_1^2}{\mu_1^2} \int_{0}^{\infty} \sum_{j=5}^{8} \frac{(2+\nu_1)m_{2j}^2 - \beta^2}{p_{2j}^2} R_{2j}(\beta) \beta e^{m_{2j}y} \sin\beta x d\beta$$

$$+ \frac{\lambda_1^2}{\mu_1^2} x \, w(x,y) \ , \quad (x>0, \ y<0) \ , \tag{44}$$

$$u(x,y) = \frac{2}{\pi} \frac{\lambda_2^2}{\mu_2^2} \int_0^\infty \sum_{j=1}^4 \frac{(2+\nu_2)m_{3j}^2 - \beta^2}{p_{3j}^2} R_{3j}(\beta)\beta e^{m_{3j}y} \sin\beta x \, d\beta$$

$$+ \frac{\lambda_2^2}{\mu_2^2} x \, w(x,y) \; , \quad (x>0, \; y<0) \; , \tag{45}$$

$$v(x,y) = -\frac{i}{2\pi} \frac{\lambda_1^2}{\mu_1^2} \int_{-\infty}^\infty \sum_{j=1}^4 \frac{\alpha}{p_{1j}^2} R_{1j}(\alpha)(m_{1j}^2 + \nu_1\alpha^2)e^{m_{1j}x - i\alpha y} \, d\alpha$$

$$- \frac{2}{\pi} \frac{\lambda_1^2}{\mu_1^2} \int_0^\infty \sum_{j=5}^8 \frac{m_{2j}}{p_{2j}^2} R_{2j}(\beta)(\beta^2 + \nu_1 m_{2j}^2)e^{m_{2j}y} \cos\beta x \, d\beta ,$$

$$(x>0, \; y<0) \; , \tag{46}$$

$$v(x,y) = -\frac{2}{\pi} \frac{\lambda_2^2}{\mu_2^2} \int_0^\infty \sum_{j=1}^4 \frac{m_{3j}}{p_{3j}^2} R_{3j}(\beta)(\beta^2 + \nu_2 m_{3j}^2)e^{m_{3j}y} \cos\beta x \, d\beta \; ,$$

$$(x>0, \; y>0) \; . \tag{47}$$

3. The Integral Equations

Referring to the general formulation of the problem given in the previous section it is seen that the first thirteen conditions (33)-(37) are homogeneous and may be used to eliminate thirteen of the fifteen unknown functions R_{ij} and A_k ($i=1,2,3$; $j=1,\ldots,4$; $k=1,2,3$). The mixed boundary conditions (38) and (39) would then give the integral equations to determine the remaining two. To derive the integral equations we first introduce the following new unknown functions which are the complements of the known crack surface tractions F_1 and F_2:

$$G_1(y) = \frac{\partial}{\partial y} u(+0,y) \; , \quad G_2(y) = \frac{\partial}{\partial y} \beta_x(+0,y) \; , \quad (y<0) \; . \tag{48}$$

From the solution given in the previous section and from (48) it may be shown that

$$G_1(y) = -\frac{i}{2\pi} \frac{\lambda_1^2}{\mu_1^2} \int_{-\infty}^\infty \sum_{j=1}^4 \frac{(1+\nu_1)\alpha^2 - p_{1j}}{p_{1j}^2} R_{1j}(\alpha)\alpha e^{-i\alpha y} \, d\alpha \; , \tag{49}$$

$$G_2(y) = -\frac{i}{2\pi} \int_{-\infty}^{\infty} \sum_{j=1}^{4} \frac{\alpha m_{1j} R_{1j}(\alpha)}{\kappa_1 p_{1j}-1} e^{-i\alpha y} d\alpha$$

$$- \frac{\kappa_1(1-\nu_1)}{4\pi} \int_{-\infty}^{\infty} \alpha^2 A_1(\alpha) e^{-i\alpha y} d\alpha \ . \tag{50}$$

By inverting (49) and (50) and by using (33)-(37) one may express all fifteen unknown functions R_{ij} and A_k in terms of G_1 and G_2. From (38b), (39b) and (48) it may be observed that

$$G_i(y) = 0, \ (i=1,2; \ -\infty<y<-d_1, \ -b_1<y<0) \ , \tag{51}$$

and (38b) and (39b) would be identically satisfied if

$$\int_{-d_1}^{-b_1} G_i(y) dy = 0, \ (i=1,2) \ . \tag{52}$$

From the formulation of the problem the conditions (38a) and (39a) may be expressed as

$$N_{xx}(+0,y) = \lim_{x \to +0} \frac{1}{2\pi} \left(\frac{\lambda_1}{\mu_1}\right)^2 \int_{-\infty}^{\infty} \sum_{j=1}^{4} \frac{\alpha^4}{p_{1j}^2} R_{1j}(\alpha) e^{m_{1j}x-i\alpha y} d\alpha$$

$$+ \frac{2}{\pi} \left(\frac{\lambda_1}{\mu_1}\right)^2 \int_{0}^{\infty} \sum_{j=5}^{8} \frac{m_{2j}^4}{p_{2j}^2} R_{2j}(\beta) e^{m_{2j}y} \cos\beta x d\beta = F_1(y) \ ,$$

$$(-d_1<y<-b_1) \ , \tag{53}$$

$$M_{xx}(+0,y) = \lim_{x \to +0} \frac{a}{h\mu_1^4} \left\{ \frac{1}{2\pi} \int_{-\infty}^{\infty} \sum_{j=1}^{4} \frac{m_{1j}^2-\nu_1\alpha^2}{\kappa_1 p_{1j}-1} R_{1j}(\alpha) e^{m_{1j}x-i\alpha y} d\alpha \right.$$

$$- \frac{i\kappa_1(1-\nu_1)^2}{4\pi} \int_{-\infty}^{\infty} \alpha r_1 A_1(\alpha) e^{r_1 x-i\alpha y} d\alpha - \frac{2}{\pi} \int_{0}^{\infty} \left[\sum_{j=5}^{8} \frac{\beta^2-\nu_1 m_{2j}^2}{\kappa_1 p_{2j}-1} R_{2j}(\beta) e^{m_{2j}y} \right.$$

$$- \frac{\kappa_1(1-\nu_1)^2}{2} \beta r_2 A_2(\beta) e^{r_2 y} \left] \cos\beta x d\beta \right\} = F_2(y), \ (-d_1<y<-b_1) \ . \tag{54}$$

-10-

If we now write R_{ij} and A_j in terms of G_1 and G_2 and take into account (51), (53) and (54) become

$$\int_{-d_1}^{-b_1} \sum_{j=1}^{2} H_{kj}(y,t)G_j(t)dt = F_k(y), \quad (k=1,2, \ -d_1<y<-b_1) , \tag{55}$$

$$H_{kj}(y,t) = \lim_{x\to+0} \{\int_{-\infty}^{\infty} B_{kj}(x,\alpha)e^{i(t-y)\alpha}d\alpha + \int_0^{\infty} C_{kj}(y,\beta)\cos\beta x d\beta\} , \tag{56}$$

where B_{kj} and C_{kj}, $(k,j=1,2)$ are known functions. The derivation of these functions are rather lengthy but quite straightforward and will not be reproduced in this paper. From the viewpoint of obtaining the correct singular behavior of G_1 and G_2 near and at the end points $y=-d_1$ and $y=-b_1$ and a sufficiently accurate solution of the system of integral equations (55), it is essential that the dominant parts of the kernels given by (56) be separated. This can be done by examining the asymptotic behavior of $B_{kj}(x,\alpha)$ and $C_{kj}(y,\beta)$, $(k,j=1,2)$, for $|\alpha|\to\infty$ and $\beta\to\infty$, respectively, by separating the asymptotic terms $B_{kj\infty}$ and $C_{kj\infty}$ and by evaluating the corresponding integrals in closed form. A key step in this process is the determination of the roots of the characteristic equations (12)-(14) (see, for example, [10]). It may then be shown that for large values of $|\alpha|$ and β the roots have the form

$$m_{1j} = -|\alpha|(1 + \frac{p_{1j}}{2\alpha^2} - \frac{p_{1j}^2}{8\alpha^4} + \ldots), \quad (j=1,\ldots,4) , \tag{57}$$

$$m_{2j} = \beta(1 + \frac{p_{2j}}{2\beta^2} - \frac{p_{2j}^2}{8\beta^4} + \ldots) , \quad (j=5,\ldots,8) , \tag{58}$$

$$m_{3j} = -\beta(1 + \frac{p_{3j}}{2\beta^2} - \frac{p_{3j}^2}{8\beta^4} + \ldots) , \quad (j=1,\ldots,4) . \tag{59}$$

Also, from (26)-(28) it may be seen that for $|\alpha|\gg1$ and $\beta\gg1$ we have

$$r_1 = -|\alpha|(1 + \frac{1}{\kappa_1(1-\nu_1)\alpha^2} - \ldots), \ r_2 = \beta(1 + \frac{1}{\kappa_1(1-\nu_1)\beta^2} - \ldots) ,$$

$$r_3 = -\beta(1 + \frac{1}{\kappa_2(1-\nu_2)\beta^2} - \ldots) . \tag{60a-c}$$

After evaluating the dominant kernels the integral equations (55) may be expressed as

$$\int_{-d_1}^{-b_1} \{[k_{1s}(y,t)+k_{11}(y,t)]G_1(t)+k_{12}(y,t)G_2(t)\}dt = 2\pi F_1(y), \quad (-d_1<y<-b_1) ,$$

(61)

$$(1-\nu_1^2)\int_{-d_1}^{-b_1} \{k_{21}(y,t)G_1(t)+[k_{2s}(y,t)+k_{22}(y,t)]G_2(t)\}dt$$

$$= 2\pi \frac{h\mu_1^4}{a} F_2(y), \quad (-d_1<y<-b_1) ,$$

(62)

where

$$k_{1s}(y,t)=k_{2s}(y,t)= \frac{1}{t-y} - (\frac{c_1(3c_3+2c_4)+2c_2c_5}{c_1c_6}) \frac{1}{t+y} + (\frac{6c_3}{c_6}) \frac{y}{(t+y)^2}$$

$$- (\frac{4c_3}{c_6}) \frac{y^2}{(t+y)^3} ,$$

(63)

$$c_1=-3+\nu_2-(1+\nu_1)E_2/E_1 , \quad c_2=1+E_2/E_1 , \quad c_3=1+\nu_2-(1+\nu_1)E_2/E_1 ,$$

$$c_4=-\nu_2+\nu_1 E_2/E_1 , \quad c_5=3-\nu_2-(3-\nu_1)E_2/E_1 , \quad c_6=1+\nu_2+(3-\nu_1)E_2/E_1$$

(64)

and the kernels $k_{ij}(y,t)$, $(i,j=1,2)$ are bounded in the closed interval $-d_1\le(y,t)\le-b_1$ (including the case $b_1=0$). The dominant or singular kernels k_{is} and the bounded kernels k_{ij}, $(i,j=1,2)$ are obtained from the integrals of the form:

$$k_{1s}(y,t) = \lim_{x\to+0} \{\int_{-\infty}^{\infty} B_{11\infty}(x,\alpha)e^{i(t-y)\alpha}d\alpha + \int_{0}^{\infty} C_{11\infty}(y,\beta)\cos\beta x d\beta\},$$

(65)

$$k_{1j}(y,t) = \int_{-\infty}^{\infty} [B_{1j}(0,\alpha)-B_{1j\infty}(0,\alpha)]e^{i(t-y)\alpha}d\alpha$$

$$+ \int_{0}^{\infty} [C_{1j}(y,\beta)-C_{1j\infty}(y,\beta)]d\beta , \quad (j=1,2) .$$

(66)

The important point to observe about the integral equations is that, as in the homogeneous shells, only the diagonal kernels contain singular terms and the dominant kernels k_{1s} and k_{2s} corresponding to membrane and bending loads are identical. This physically expected result is possible again because of the use of a transverse shear theory in formulating the problem. Also, it can easily be shown that the dominant kernel k_{1s} found for the nonhomogeneous shell in this study is identical to that obtained for two dissimilar bonded half planes with a crack perpendicular to the interface under plane stress conditions which is given in [14]. The plane stress problem is, of course, a limiting case of the shell problem and this, too, is the expected result.

4. The Stress Intensity Factor

After solving the integral equations, clearly any desired field quantity may be obtained from integrals with appropriate kernels having G_1 and G_2 as the density functions. For example, it may be observed that before going to the limit, (53) and (54) give $N_{xx}(x,y)$ and $M_{xx}(x,y)$ everywhere in the shell. In particular we note that (55) or (61) and (62) are valid for x=0 outside as well as within the cut $-d_1 < y < -b_1$. Thus, through a simple asymptotic analysis of (61) and (62) one can obtain the stress intensity factors at the crack tips which, for b>0, are defined by (Fig. 1b)

$$k_1(-b,x_3) = \lim_{x_2 \to -b+0} \sqrt{2(x_2+b)}\ \sigma_{11}(0,x_2,x_3)\ , \tag{67}$$

$$k_1(-d,x_3) = \lim_{x_2 \to -d-0} \sqrt{-2(x_2+d)}\ \sigma_{11}(0,x_2,x_3)\ . \tag{68}$$

In the shells the in-plane stress components are obtained by combining membrane and bending stresses as follows:

$$\sigma_{ij}(x_1,x_2,x_3) = \sigma_{ij}^m + \sigma_{ij}^b\ , \quad (i,j=1,2) \tag{69}$$

$$\sigma_{ij}^m = \frac{1}{h} N_{ij}(x_1,x_2)\ , \quad \sigma_{ij}^b = \frac{12x_3}{h^3} M_{ij}(x_1,x_2)\ , \quad (i,j=1,2)\ . \tag{70}$$

-13-

Now for b>0 from (61)-(63) it is seen that the dominant kernels k_{1s} and k_{2s} consist of $(t-y)^{-1}$ only and hence the solution of the integral equations may be expressed as [15]

$$G_j(y) = \frac{P_j(y)}{[-(y+d_1)(y+b_1)]^{1/2}} , \quad (j=1,2; \ -d_1<y<-b_1)$$

$$(71)$$

where P_1 and P_2 are unknown bounded functions. By substituting from Appendix A and (71) into (61) and (62) and using (67)-(70), it can be shown that

$$k_1(-b,x_3) = -\frac{E_1}{2} \lim_{x_2 \to -b-0} \sqrt{-2(x_2+b)} \frac{\partial}{\partial x_2} [u_1(+0,x_2)+x_3\beta_{11}(+0,x_2)]$$

$$= -\frac{E_1}{2} \sqrt{a} [P_1(-b_1) + \frac{x_3}{a} P_2(-b_1)] ,$$

$$(72)$$

$$k_1(-d,x_3) = \frac{E_1}{2} \lim_{x_2 \to -d+0} \sqrt{2(x_2+d)} \frac{\partial}{\partial x_2} [u_1(+0,x_2)+x_3\beta_{11}(+0,x_2)]$$

$$= \frac{E_1}{2} \sqrt{a} [P_1(-d_1) + \frac{x_3}{a} P_2(-d_1)] .$$

$$(73)$$

In the case of b=0 from (63) it is seen that the dominant part of the kernel is a generalized Cauchy kernel, that is it contains, in addition to $(t-y)^{-1}$, terms which become unbounded as the variables y and t approach the end point $-b_1=0$ (Fig. 1b). The contribution of these terms to the singular behavior of the solution at y=0 can be studied by assuming the solution of the integral equations (61) and (62) as

$$G_j(y) = S_j(y)(-y)^\gamma(y+d_1)^\omega , \quad (-1<\text{Re}(\gamma,\omega)<0) ,$$

$$(74)$$

and by following the function theoretic method (see, for example, [14] and [15]). Thus, by substituting from (74) into (61) and (62), the characteristic equations giving γ and ω may be obtained as follows:

$$\cos\pi\gamma - \frac{2c_3}{c_6} \gamma(\gamma+2) - (\frac{3c_3+2c_4}{c_6} + \frac{2c_2c_5}{c_1c_6}) = 0 ,$$

$$(75)$$

-14-

$$\cos \pi \omega = 0 \quad . \tag{76}$$

At the crack tip $y=-d_1$ which is embedded in a homogeneous medium (76) gives $\omega=-1/2$. The characteristic equation (75) found for γ is identical to that given in [14] for the plane stress case and its examination would show that for all material combinations the equation has only one root satisfying $-1<\mathrm{Re}(\gamma)<0$ and this root is always real. In [14] it was found that for the plane problem in the small neighborhood of the singular point $y=0$ located at the interface the stress state has the form

$$\sigma_{ij}(r,\theta) \cong \frac{k_1}{\sqrt{2}} r^\gamma f_{ij}(\theta) \quad , \quad i,j=r,\theta) \quad , \tag{77}$$

where r and θ are the polar coordinates and the functions f_{ij} are dependent on the bimaterial constants E_k, ν_k, (k=1,2) and are given in [14]. The constant k_1 is again defined as the stress intensity factor and is obtained from the calculated values of $\sigma_{\theta\theta}(r,0)$ by normalizing $f_{\theta\theta}(0)=1$. Thus, in the present shell problem the stress intensity factor at the crack tip $y=0$ may be defined as

$$k_1(0,x_3) = \lim_{x_2 \to +0} \sqrt{2} \, x_2^{-\gamma} \sigma_{11}(0,x_2,x_3) \quad . \tag{78}$$

To evaluate the stress intensity factor $k_1(0,x_3)$ the asymptotic expression of σ_{11} for $x_2>0$ is needed. This can again be obtained in terms of G_1 and G_2 from the basic formulation of the shell given in this paper. After somewhat lengthy but straightforward analysis it may be shown that

$$k_1(0,x_3) = -\frac{E_2}{\sqrt{2}} \left(\frac{3c_6+c_1+2\gamma(c_1+c_6)}{c_1 c_6 \sin \pi \gamma}\right) \lim_{x_2 \to +0} (-x_2)^{-\gamma} \frac{\partial}{\partial x_2} [u_1(+0,x_2)$$

$$+ x_3 \beta_{11}(+0,x_2)]$$

$$= - E_2 a^{-\gamma} \left(\frac{3c_6+c_1+2(c_1+c_6)\gamma}{c_1 c_6 \sin \pi \gamma}\right)[S_1(0) + \frac{x_3}{a} S_2(0)] \quad , \tag{79}$$

Also, at the crack tip $x_2=-d$ the expression

$$k_1(-d,x_3) = \frac{E_1}{2} \lim_{x_2 \to -d+0} \sqrt{2(x_2+d)} \frac{\partial}{\partial x_2} [u_1(+0,x_2) + x_3\beta_{11}(+0,x_2)] \quad (80)$$

is still valid and by using (48) and (71) can be written as

$$k_1(-d,x_3) = \frac{E_1}{2^{\frac{1}{2}-\gamma}} \sqrt{a} [S_1(-d_1) + \frac{x_3}{a} S_2(-d_1)] . \quad (81)$$

5. Results

For $b>0$ the integral equations (61) and (62) subject to (52) may easily be solved by using the Gauss-Chebyshev quadrature formulas described in, for example, [14] by assuming the solution in the form (71). The stress intensity factors may then be obtained from (72) and (73). From (72) and (73) it is seen that the values of the bounded functions P_1 and P_2 at the end points $-d_1$ and $-b_1$ are associated with respectively the membrane and the bending components of the stresses near the crack tips. For the pressurized shell shown in Fig. 1b, one can, therefore, define the following normalized stress intensity factors:

$$k_m(r_j) = \frac{k_1(r_j,0)}{(pR_i/h)\sqrt{a}} , \quad k_b(r_j) = \frac{k_1(r_j,h/2)-k_1(r_j,0)}{(pR_i/h)\sqrt{a}} , \quad (82)$$

where $r_1=-b$ and $r_2=-d$ and the stress intensity factors $k_1(r_j,x_3)$, (j=1,2) are given by (72) and (73). For b=0 the definition of the normalized stress intensity factors at $r_2=-d$ would remain the same as in (82) and may be obtained from (81). At $r_1=-b=0$ we have

$$k_m(0) = \frac{k_1(0,0)}{(pR_i/h)a^{-\gamma}} , \quad k_b(0) = \frac{k_1(0,h/2)-k_1(0,0)}{(pR_i/h)a^{-\gamma}} \quad (83)$$

where k_1 is given by (79). In (82) and (83) R_i is the inner radius of the cylinder.

The reinforced shell shown in Fig. 1a is considered as an example. The main shell having properties E_1,ν_1 is steel and the reinforcing shell

is a fiber reinforced composite. The dimensions of four different
cylinders used in the analysis are shown in Table 1. The table also
shows the elastic constants E_2, ν_2 of the equivalent homogeneous shell
shown in Fig. 1b. The derivation of E_2, ν_2 and the solution of the nonhomo-
geneous shell in the absence of any cracks giving the crack surface
loads F_1 and F_2 are given in Appendix B (see, (61) and (62)). It should
be noted that F_1 and F_2 are functions of $y = x_2/a$. One may also note that
the effective elastic constants E_2, ν_2 as well as F_1, F_2 are dependent on
the axis1 constraint in the cylinder. In the examples it is assumed that
either there is no axial constraint (labeled as a cylinder with "open
ends") or the ends of the cylinder are "closed", corresponding to the
total axial force in the internally pressurized cylinder $P=0$ and $P=\pi R_i^2 p$,
respectively (Eq. B6).

Table 1. Dimensions and the effective material constants
(E_2, ν_2) of the composite shell used in numerical
examples.

Shell #		1	2	3	4
E_1	{psi	3×10^7	3×10^7	3×10^7	3×10^7
	{GPa	207	207	207	207
ν_1		0.3	0.3	0.3	0.3
E' (reinforcing shell){	psi	2×10^7	2×10^7	2×10^7	2×10^7
	GPa	138	138	138	138
ν' (reinforcing shell)		0.1	0.1	0.1	0.1
h (thickness)	{in.	1	0.615	0.5	0.404
	{m	0.0254	0.0156	0.0127	0.0103
R (mean radius)	{in.	100	23.6925	17.75	11.798
	{m	2.54	0.6018	0.4509	0.2997
h_2 (reinforcing shell){	in.	1	0.615	0.5	0.404
	m	0.0254	0.0156	0.0127	0.0103
R/h		100	38.524	35.5	29.203
Open Ends:					
E_2	{psi	50.2×10^6	49.72×10^6	49.66×10^6	49.48×10^6
	{GPa	346	343	342	341
ν_2		0.2214	0.2174	0.2168	0.2153
$-\gamma$		0.449518	0.450677	0.450827	0.451265
Closed Ends:					
E_2	{psi	50.06×10^6	49.37×10^6	49.28×10^6	49.03×10^6
	{GPa	345	340	340	338
ν_2		0.2272	0.2321	0.2327	0.2345
$-\gamma$		0.440538	0.450728	0.450886	0.451323

For these two cases the values of E_2 and ν_2 calculated from Appendix B are given in Table 1.

The stress intensity factors obtained by using dimensions and properties of four different shells shown in Table 1 are given in Tables 2-5. The normalized stress intensity factors given in the tables are defined by (82) for b>0 (or c>a) and by (81) and (83) for b=0 (or c=a). One may observe that as the relative distance of the crack to the interface c/a increases the stress intensity factors approach those given for the homogeneous shell [9]. The tables also show that the membrane component k_m of the stress intensity factor (which is by far the dominant part) decreases with the decreasing crack distance to the boundary. Even though the results found for "open" and "closed" ended cylinders are different, for the axial through crack geometry under consideration the differences seem to be relatively insignificant. It should be emphasized that the tables show the stress intensity factors normalized with respect to $(pR_i/h)\sqrt{a}$ which is the corresponding flat plate (or plane stress) result under the same membrane loading as the shell. Thus the variation in the stress intensity factors as a function of a/h and R/h is entirely due to curvature and thickness effects.

In Tables 2-5 the membrane and bending components of the stress intensity factors are given separately. In all cases, the calculated bending components were such that the stress intensity factors on the outside surface $x_3=h/2$ were greater than that on the inside surface. Figures 2-5 show the stress intensity factor $k_1(c_i,h/2)$, $(c_i=-d,-b,0)$ obtained from (72), (73), (79) and (81) for some selected shell-crack geometries. The effect of reinforcement may be clearly observed from Figures 2 and 3. The asymptotic behavior of $k_1(-b,h/2)$ as c→a is due to different definitions of k_1 for b>0 and b=0 as given by (67) and (78). For these two cases the cleavage stress in the close neighborhood of the crack tip may be expressed as (Fig. 1b)

$$\sigma_{11}(0,x_2) \cong \frac{k_1(-b,h/2)}{\sqrt{2r}} , \quad (r=x_2+b,\ b>0,\ x_2>-b) , \qquad (84)$$

$$\sigma_{11}(0,x_2) \cong \frac{k_1(0,h/2)}{\sqrt{2}\ r^{-\gamma}} = \frac{k_1(0,h/2)r^{\frac{1}{2}+\gamma}}{\sqrt{2r}} \ , \ (r=x_2>0, \ b=0). \tag{85}$$

Thus, since $1/2+\gamma>0$ (see Table 1), the stress intensity factor defined on the basis of the conventional square root singularity becomes

$$\lim_{\substack{b\to 0}} k_1(-b,\ h/2) = \lim_{\substack{r\to 0 \\ b\to 0}} \sqrt{2r}\ \sigma_{11}(0,x_2) = \lim_{\substack{r\to 0}} k_1(0,h/2)r^{\frac{1}{2}+\gamma} = 0 \ . \tag{86}$$

Figures 4 and 5 show the normalized stress intensity factors on the outside surface $x_3=h/2$ for $b=0$ obtained from (79) and (81). Here, too, it may be seen that even for a relatively very shallow shell (shell no. 1), there is considerable curvature and thickness effect.

References

1. G.C. Sih, ed. Plates and Shells with Cracks, Noordhoff International Publishing, Leyden, The Netherlands, 1977.

2. E. Reissner, "On Bending of Elastic Plates", Quarterly of Applied Mathematics, Vol. 5, pp. 55-68, 1947.

3. J.K. Knowles and N.M. Wang, "On Bending of Elastic Plates Containing a Crack", J. Math. and Phys., Vol. 39, pp. 223-236, 1960.

4. F. Delale and F. Erdogan, "The Effects of Transverse Shear in a Cracked Plate under Skew-Symmetric Loading", J. Appl. Mech., Vol. 46, Trans. ASME, pp. 618-624, 1979.

5. O.S. Yahsi and F. Erdogan, "A Cylindrical Shell with an Arbitrarily Oriented Crack", Int. J. Solids Structures, Vol. 19, pp. 955-972, 1983.

6. H. Boduroglu and F. Erdogan, "Internal and Edge Cracks in a Plate of Finite Width under Bending", J. Appl. Mech., Vol. 50, Trans. ASME, pp. 621-629, 1983.

7. F. Erdogan and O.S. Yahsi, "A Cylindrical Shell with a Stress-Free End which Contains an Axial Part-Through or Through Crack", Int. J. Engng. Sci., Vol. 23, pp. 1215-1237, 1985.

References (cont.)

8. O.S. Yahsi and F. Erdogan, "A Pressurized Cylindrical Shell with a Fixed End Which Contains an Axial Part-Through or Through Crack", Int. J. of Fracture, Vol. 28, pp. 161-187, 1985.

9. S. Krenk, "Influence of Transverse Shear on an Axial Crack in a Cylindrical Shell", Int. J. of Fracture, Vol. 14, pp. 123-143, 1978.

10. F. Delale and F. Erdogan, "Transverse Shear Effect in a Circumferentially Cracked Cylindrical Shell", Quarterly of Applied Mathematics, Vol. 37, pp. 239-258, 1979.

11. F. Delale and F. Erdogan, "Effect of Transverse Shear and Material Orthotropy in a Cracked Spherical Cap", Int. J. Solids Structures, Vol. 15, pp. 907-926, 1979.

12. F. Delale and F. Erdogan, "The Crack Problem in a Specially Orthotropic Shell with Double Curvature", Engng. Fracture Mech., Vol. 18, pp. 529-544, 1983.

13. M.E. Duncan and J.L. Sanders, Jr., "The Effect of Circumferential Stiffener on the Stress in a Pressurized Cylindrical Shell with a Longitudinal Crack", Int. J. of Fracture Mechanics, Vol. 5, pp. 133-155, 1969.

14. T.S. Cook and F. Erdogan, "Stresses in Bonded Materials with a Crack Perpendicular to the Interface", Int. J. Engng. Sci., Vol. 10, pp. 667-697, 1972.

15. N.I. Muskhelishvili, Singular Integral Equations, Noordhoff, Groningen, The Netherlands, 1953.

16. S. Timoshenko and S. Woinowsky-Krieger, Theory of Plates and Shells, McGraw-Hill, New York, 1959.

Table 2. Membrane component k_m of the normalized stress intensity factor in a pressurized composite shell with open ends which contains an axial crack.

Shell No.	c/a a/h	$k_m(-b)$					$k_m(-d)$				
		1.0	1.1	1.5	2	10	1.0	1.1	1.5	2	10
1	1	1.812	0.695	0.778	0.809	0.978	0.789	0.798	0.820	0.839	0.990
	2	1.878	0.722	0.819	0.864	1.050	0.841	0.852	0.885	0.916	1.049
	3	1.973	0.759	0.874	0.934	1.082	0.903	0.918	0.960	0.998	1.079
	10	3.097	1.203	1.447	1.534	1.542	1.442	1.472	1.532	1.549	1.542
2	1	1.849	0.721	0.812	0.851	1.041	0.830	0.840	0.869	0.895	1.041
	2	1.998	0.782	0.900	0.962	1.100	0.929	0.944	0.988	1.027	1.097
	3	2.198	0.862	1.010	1.088	1.175	1.042	1.061	1.113	1.152	1.176
	10	4.426	1.730	2.057	2.101	2.096	1.999	2.036	2.091	2.096	2.096
3	1	1.853	0.724	0.817	0.867	1.046	0.835	0.845	0.875	0.902	1.049
	2	2.013	0.788	0.910	0.973	1.106	0.940	0.956	1.000	1.039	1.104
	3	2.227	0.876	1.027	1.107	1.189	1.058	1.078	1.131	1.170	1.189
	10	4.581	1.790	2.125	2.164	2.161	2.062	2.100	2.155	2.160	2.161
4	1	1.866	0.733	0.829	0.871	1.057	0.848	0.860	0.890	0.919	1.058
	2	2.053	0.809	0.937	1.004	1.124	0.969	0.985	1.031	1.071	1.123
	3	2.304	0.912	1.073	1.156	1.225	1.102	1.123	1.177	1.214	1.226
	10	4.980	1.947	2.297	2.327	2.326	2.225	2.264	2.319	2.324	2.326

Table 3. Bending component k_b of the normalized stress intensity factor in a pressurized composite shell with <u>open</u> ends which contains an axial crack.

Shell No.	c/a a/h	$k_m(-b)$					$k_m(-d)$				
		1.0	1.1	1.5	2	10	1.0	1.1	1.5	2	10
1	1	0.005	0.002	0.008	0.014	0.039	0.015	0.016	0.020	0.024	0.037
	2	0.047	0.021	0.035	0.044	0.046	0.042	0.044	0.050	0.055	0.043
	3	0.087	0.042	0.062	0.075	0.064	0.069	0.072	0.078	0.082	0.064
	10	0.225	0.134	0.202	0.212	0.197	0.191	0.196	0.204	0.203	0.198
2	1	0.033	0.015	0.026	0.034	0.043	0.043	0.035	0.041	0.046	0.039
	2	0.101	0.046	0.069	0.081	0.071	0.076	0.079	0.085	0.089	0.070
	3	0.154	0.074	0.108	0.123	0.110	0.111	0.114	0.121	0.123	0.110
	10	0.164	0.124	0.211	0.207	0.198	0.200	0.202	0.207	0.203	0.198
3	1	0.037	0.017	0.027	0.036	0.044	0.036	0.038	0.043	0.047	0.040
	2	0.107	0.050	0.080	0.086	0.074	0.079	0.082	0.089	0.092	0.074
	3	0.161	0.078	0.117	0.128	0.114	0.115	0.119	0.125	0.127	0.114
	10	0.148	0.108	0.197	0.200	0.192	0.194	0.197	0.201	0.197	0.193
4	1	0.046	0.021	0.032	0.043	0.047	0.041	0.043	0.049	0.053	0.042
	2	0.120	0.055	0.082	0.096	0.083	0.088	0.091	0.097	0.099	0.082
	3	0.176	0.086	0.124	0.140	0.126	0.126	0.129	0.135	0.136	0.125
	10	0.102	0.099	0.186	0.172	0.172	0.178	0.179	0.181	0.177	0.172

Table 4. Membrane component k_m of the normalzied stress intensity factor in a pressurized composite shell with closed ends which contains an axial crack.

Shell No.	c/a a/c	$k_m(-b)$					$k_m(-d)$				
		1.0	1.1	1.5	2	10	1.0	1.1	1.5	2	10
1	1	1.909	0.735	0.820	0.848	0.985	0.828	0.836	0.857	0.874	0.994
	2	1.969	0.759	0.856	0.897	1.047	0.872	0.883	0.912	0.938	1.047
	3	2.059	0.795	0.907	0.959	1.081	0.929	0.942	0.979	1.011	1.078
	10	3.158	1.229	1.458	1.533	1.542	1.448	1.475	1.531	1.546	1.542
2	1	1.932	0.760	0.851	0.887	1.039	0.865	0.874	0.900	0.923	1.042
	2	2.074	0.818	0.932	0.986	1.099	0.954	0.968	1.006	1.039	1.097
	3	2.265	0.897	1.037	1.104	1.176	1.059	1.077	1.123	1.156	1.176
	10	4.446	1.750	2.059	2.098	2.096	2.001	2.036	2.089	2.095	2.096
3	1	1.936	0.764	0.856	0.892	1.044	0.869	0.879	0.905	0.929	1.046
	2	2.087	0.825	0.942	0.997	1.106	0.964	0.978	1.018	1.051	1.104
	3	2.293	0.910	1.053	1.122	1.189	1.075	1.093	1.139	1.173	1.189
	10	4.593	1.810	2.126	2.161	2.161	2.063	2.100	2.153	2.159	2.161
4	1	1.944	0.773	0.867	0.905	1.055	0.882	0.892	0.920	0.944	1.056
	2	2.122	0.846	0.968	1.026	1.124	0.990	1.006	1.047	1.080	1.123
	3	2.363	0.946	1.098	1.169	1.226	1.117	1.136	1.184	1.216	1.226
	10	4.977	1.966	2.297	2.324	2.326	2.227	2.265	2.318	2.324	2.326

Table 5. Bending component k_b of the normalized stress intensity factor in a pressurized composite shell with closed ends which contains an axial crack.

Shell No.	c/a, a/h	$-k_b(-b)$					$k_b(-d)$				
		1.0	1.1	1.5	2	10	1.0	1.1	1.5	2	10
1	1	0.010	0.003	0.010	0.014	0.034	0.015	0.016	0.019	0.022	0.032
	2	0.051	0.023	0.035	0.042	0.045	0.041	0.042	0.047	0.051	0.042
	3	0.091	0.042	0.061	0.072	0.061	0.067	0.069	0.074	0.078	0.064
	10	0.230	0.135	0.199	0.209	0.197	0.190	0.195	0.203	0.203	0.198
2	1	0.038	0.016	0.026	0.033	0.040	0.033	0.034	0.038	0.041	0.037
	2	0.105	0.048	0.068	0.079	0.071	0.074	0.076	0.082	0.085	0.070
	3	0.158	0.076	0.107	0.120	0.110	0.109	0.112	0.118	0.119	0.110
	10	0.171	0.125	0.219	0.205	0.198	0.199	0.202	0.207	0.203	0.198
3	1	0.042	0.019	0.027	0.035	0.041	0.034	0.036	0.040	0.044	0.038
	2	0.111	0.051	0.072	0.083	0.074	0.078	0.079	0.085	0.088	0.074
	3	0.165	0.080	0.111	0.125	0.114	0.114	0.117	0.122	0.123	0.114
	10	0.156	0.119	0.203	0.200	0.192	0.195	0.197	0.201	0.197	0.193
4	1	0.050	0.022	0.033	0.041	0.045	0.039	0.042	0.046	0.050	0.041
	2	0.125	0.058	0.081	0.092	0.083	0.086	0.089	0.092	0.096	0.083
	3	0.180	0.088	0.123	0.137	0.126	0.124	0.127	0.134	0.134	0.125
	10	0.112	0.101	0.184	0.179	0.172	0.179	0.180	0.181	0.177	0.172

APPENDIX A
Normalized quantities used in the formulation
of the composite shell problem

$$x = x_1/a, \quad y = x_2/a, \quad z = x_3/a, \quad b_1 = b/a, \quad c_1 = c/a, \quad d_1 = d/a \,, \tag{A1}$$

$$u = u_1/a, \quad v = u_2/a, \quad w = u_3/a, \quad \beta_x = \beta_1, \quad \beta_y = \beta_2 \,, \tag{A2}$$

$$\phi(x,y) = \begin{cases} F(x_1,x_2)/(E_1 ha^2) \,, & y < 0 \,, \\[2mm] F(x_1,x_2)/(E_2 ha^2) \,, & y > 0 \,, \end{cases} \tag{A3}$$

$$\sigma_{\alpha\beta}(x,y,z) = \begin{cases} \sigma_{ij}/E_1 \,, & y < 0 \,, \\[2mm] \sigma_{ij}/E_2 \,, & y > 0 \,, \end{cases} \quad (\alpha,\beta=x,y;\ i,j=1,2) \,, \tag{A4}$$

$$N_{\alpha\beta}(x,y) = \begin{cases} N_{ij}/(E_1 h) \,, & y < 0 \,, \\[2mm] N_{ij}/(E_2 h) \,, & y > 0 \,, \end{cases} \quad (\alpha,\beta=x,y;\ i,j=1,2) \,, \tag{A5}$$

$$M_{\alpha\beta}(x,y) = \begin{cases} M_{ij}/(E_1 h^2) \,, & y < 0, \\[2mm] M_{ij}/(E_2 h^2) \,, & y > 0, \end{cases} \quad (\alpha,\beta=x,y;\ i,j=1,2) \,, \tag{A6}$$

$$V_\gamma(x,y) = \begin{cases} V_k/(B_1 h) \,, & y < 0 \,, \\[2mm] V_k/(B_2 h) \,, & y > 0 \,, \end{cases} \quad (\gamma=x,y;\ k=1,2) \,, \tag{A7}$$

$$B_i = 5E_i/(12(1+\nu_i)) \,, \quad \kappa_i = E_i/(B_i \mu_i^4) \,, \quad (i=1,2) \,, \tag{A8}$$

$$\mu_i^4 = 12(1-\nu_i^2)a^2/h^2 \,, \quad \lambda_i^4 = 12(1-\nu_i^2)a^4/(R^2 h^2) \,, \quad (i=1,2) \,. \tag{A9}$$

APPENDIX B

Solution of the uncracked composite shell problem

The first problem here is the determination of elastic constants E_2 and ν_2 of a cylindrical shell which has the same stiffness as a long layered cylinder (see Fig. 1a and 1b for $x_2 \gg 0$). The second problem is the solution of the bonded shells shown in Fig. 1b in the absence of any cracks in order to determine the crack surface tractions $F_1(y) = N_{11}(0,x_2)/(hE_1)$ and $F_2(y) = M_{11}(0,x_2)/(h^2 E_1)$ which are used in the perturbation solution of the cracked shell as the input functions. In the first problem we use the following basic (axisymmetric) solution of a thick-walled cylinder under plane strain conditions:

$$\sigma_{rr}(r) = A + \frac{B}{r^2} \ , \quad \sigma_{\theta\theta}(r) = A - \frac{B}{r^2} \ ,$$

$$w(r) = \frac{1-\nu-2\nu^2}{E} Ar - \frac{1+\nu}{E}\frac{B}{r} - \nu\varepsilon_{zz}r \ , \quad (a<r<b) \ , \qquad \text{(B1a-c)}$$

where A and B are unknown constants and w is the radial displacement. For the three cylinders we have (Fig. 1)

$$a_1 = R_i \ , \quad b_1 = R_i + h \ , \quad A = A_1 \ , \quad B = B_1 \ , \quad \nu = \nu_1 \ , \quad E = E_1 \ , \qquad \text{(B2)}$$

$$a_2 = R_i + h \ , \quad b_2 = R_i + h + h_2 \ , \quad A = A_2 \ , \quad B = B_2 \ , \quad \nu = \nu' \ , \quad E = E' \ , \qquad \text{(B3)}$$

$$a_3 = R_i \ , \quad b_3 = R_i + h \ , \quad A = A_3 \ , \quad B = B_3 \ , \quad \nu = \nu_2 \ , \quad E = E_2 \ , \qquad \text{(B4)}$$

where the dimensions R_i, h, h_2 and the elastic constants E_1, ν_1, E' and ν' are known. The boundary and continuity conditions

$$\sigma_{1rr}(a_1) = -p \ , \quad \sigma_{2rr}(b_2) = 0, \quad \sigma_{1rr}(b_1) = \sigma_{2rr}(a_2) \ ,$$

$$w_1(b_1) = w_2(a_2) \ , \quad \sigma_{3rr}(a_3) = -p \ , \quad \sigma_{3rr}(b_3) = 0 \qquad \text{(B5)}$$

are used to eliminate A_i and B_i, (i=1,2,3). Additional information needed to account for ε_{zz} is

$$\varepsilon_{zz} = (\sigma_{zz} - \nu\sigma_{rr} - \nu\sigma_{\theta\theta})/E \ , \quad \int_A \sigma_{zz} dA = P \qquad \text{(B6a,b)}$$

where P is the total axial force. If the cylinder is fully constrained $\varepsilon_{zz}=0$, if there is no axial constraint, P=0 and, if the ends of the cylinder are closed and if it is subjected to an internal pressure p, then $P = \pi R_1^2 p$. In this problem it is assumed that the cylinders 1 and 2 are fully bonded along $r=b_1=a_2$ giving $\varepsilon_{1zz}=\varepsilon_{2zz}$.

The two shells are said to be equivalent if

$$\varepsilon_{3zz} = \varepsilon_{1zz} \ , \quad w_3(R) = w_1(R) \ , \qquad \text{(B7a,b)}$$

where $R = R_i + h/2$. After eliminating A_i and B_i (i=1,2,3), (B7a) and (B7b) would give the equivalent (or effective) elastic constants E_2 and ν_2 in terms of E_1, ν_1, E', ν', R_i, h and h_2.

The next problem is the evaluation of the stresses in the bonded shell shown in Fig. 1b in the absence of any cracks. Referring to [16] and Fig. 1b, the solution of the "open-ended" or axially unconstrained cylindrical shell problem may be expressed as

$$u_3(x_2) = \begin{cases} e^{\beta_1 x_2}(C_1\cos\beta_1 x_2 + C_2\sin\beta_1 x_2) - \dfrac{pR^2}{E_1 h} \ , & x_2 < 0 \ , \\[2mm] e^{-\beta_2 x_2}(C_3\cos\beta_2 x_2 + C_4\sin\beta_2 x_2 - \dfrac{pR^2}{E_2 h} \ , & x_2 > 0 \ , \end{cases} \qquad \text{(B8)}$$

where

$$\beta_1^4 = 3(1-\nu_1^2)/R^2 h^2 \ , \quad \beta_2^4 = 3(1-\nu_2^2)/R^2 h^2 \ , \qquad \text{(B9)}$$

and the constants $C_1,\ldots,C_4$ are determined from

$$u_3(-0) = u_3(+0) \ , \quad \frac{d}{dx_2} u_3(-0) = \frac{d}{dx_2} u_3(+0) \ , \qquad \text{(B10)}$$

$$D_1 \frac{d^2}{dx_2^2} u_3(-0) = D_2 \frac{d^2}{dx^2} u_3(+0), \quad D_1 \frac{d^3}{dx_2^3} u_3(-0) = D_2 \frac{d^3}{dx_2^3} u_3(+0), \qquad \text{(B11)}$$

$$D_1 = \frac{E_1 h^3}{12(1-\nu_1^2)} \; , \quad D_2 = \frac{E_2 h^3}{12(1-\nu_2^2)} \; . \tag{B12}$$

Note that (B11) represents the continuity of M_{22} and V_2. Equations (B8), (B10) and (B11) may be shown to reduce

$$C_1 - C_3 = pR^2(E_2 - E_1)/(hE_1 E_2) \; ,$$

$$C_1 + C_2 = (C_4 - C_3)\beta_2/\beta_1 \; ,$$

$$C_2 = -D_2 \beta_2^2 C_4/(D_1 \beta_1^2) \; ,$$

$$C_2 - C_1 = (C_4 + C_3)D_2 \beta_2^3/(D_1 \beta_1^3). \tag{B13a-d}$$

After determining $C_1, \ldots, C_4$ from (B13), by observing that [16]

$$N_{11}(x_2) = -\frac{E_1 h}{R} u_3(x_2) \; , \quad M_{11}(x_2) = -\nu_1 D_1 \frac{d^2}{dx_2^2} u_3(x_2) \; ,$$

$$(x_2 < 0) \; , \tag{B14}$$

the input functions F_1 and F_2 may be expressed as (see (38a), (39a) and Appendix A)$^{(*)}$

$$F_1(y) = \frac{1}{R} e^{\beta_1 ay}[C_1 \cos\beta_1 ay + C_2 \sin\beta_1 ay] - \frac{pR}{hE_1} \; , \quad (y < 0) \; , \tag{B15}$$

$$F_2(y) = \frac{2\nu_1 D_1 \beta_1^2}{h^2 E_1} e^{\beta_1 ay}[-C_1 \sin\beta_1 ay + C_2 \cos\beta_1 ay] \; , \quad (y < 0) \; . \tag{B16}$$

Similarly, if the ends of the pressurized composite cylinder shown in Fig. 1b are closed, following [17] we find

---

$^{(*)}$ Note that F_1 and F_2 used in the perturbation problem, correspond to the membrane and bending resultants obtained from the uncracked cylinder with the opposite sign.

$$u_3(x_2) = \begin{cases} e^{\beta_1 x_2}[B_1 \cos\beta_1 x_2 + B_2 \sin\beta_1 x_2] + (\frac{\nu_1 - 2}{2}) \frac{pR^2}{E_1 h} \ , & (x_2 < 0) \ , \\ e^{-\beta_2 x_2}[B_3 \cos\beta_2 x_2 + B_4 \sin\beta_2 x_2] + (\frac{\nu_2 - 2}{2}) \frac{pR^2}{E_2 h} \ , & (x_2 > 0) \ , \end{cases}$$

$$\text{(B17)}$$

$$F_1(y) = \frac{1}{R} e^{\beta_1 ay}(B_1 \cos\beta_1 ay + B_2 \sin\beta_1 ay) - \frac{pR}{E_1 h} \ , \quad (y < 0) \ , \qquad \text{(B18)}$$

$$F_2(y) = \frac{2\nu_1 D_1 \beta_1^2}{h^2 E_1} e^{\beta_1 ay}(-B_1 \sin\beta_1 ay + B_2 \cos\beta_1 ay) \ , \quad (y > 0) \ , \qquad \text{(B19)}$$

where $B_1, \ldots, B_4$ are obtained from the solution of the following system:

$$B_1 - B_3 = \frac{pR^2}{h}(\frac{2-\nu_1}{2E_1} - \frac{2-\nu_2}{2E_2}) \ ,$$

$$B_1 + B_2 = (B_4 - B_3)\beta_2/\beta_1 \ ,$$

$$B_2 = -B_4 D_2 \beta_2/(D_1 \beta_1) \ ,$$

$$B_2 - B_1 = (B_4 + B_3)D_2\beta_2^3/(D_1\beta_1^3) \ . \qquad \qquad \text{(B20a-d)}$$
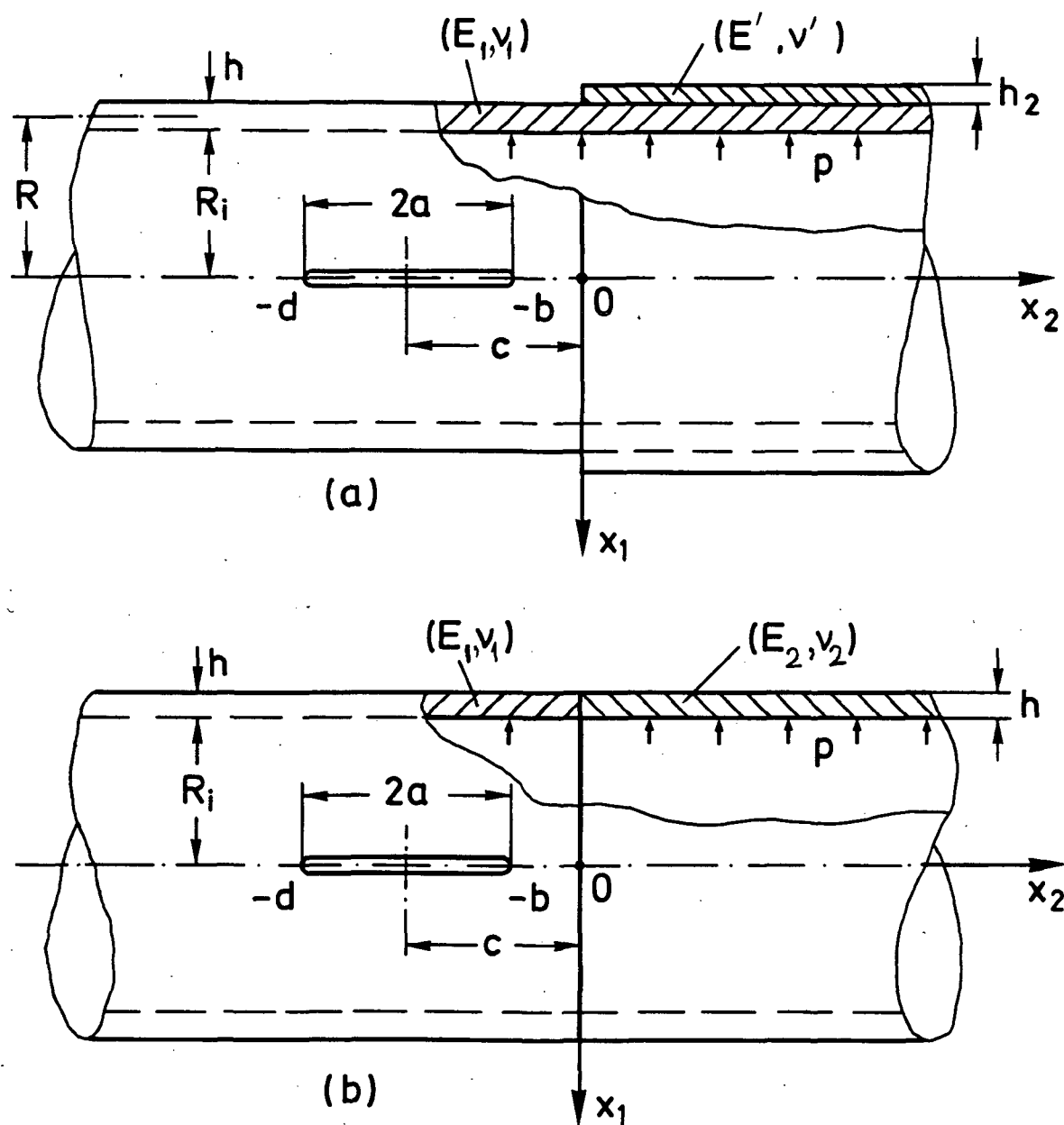
Fig. 1   Geometry and notation for a reinforced cylindrical shell con-
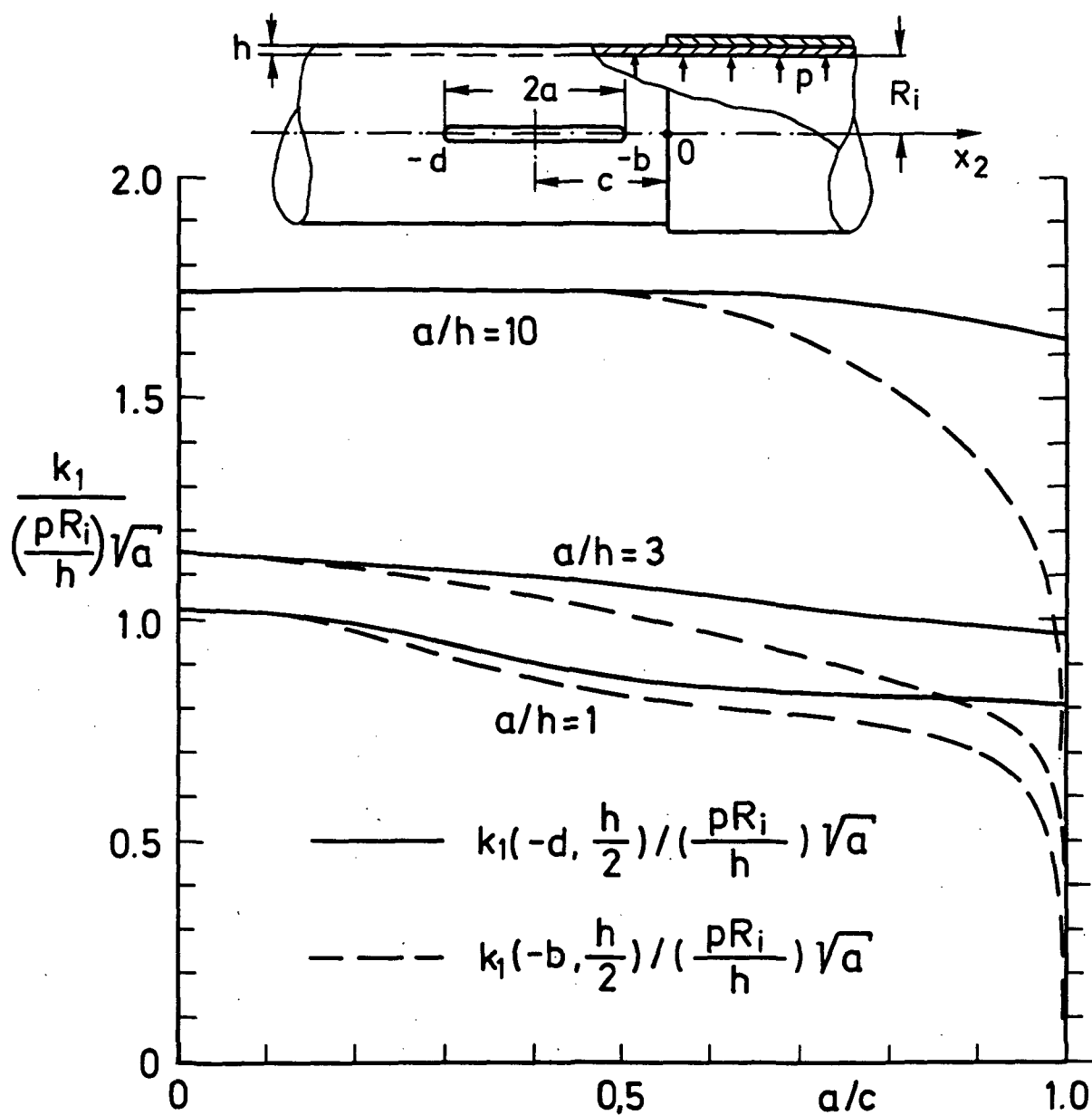   taining an axial crack.

Fig. 2   Normalized stress intensity factors on the outside surface of an "open-ended" reinforced cylindrical shell containing an axial through crack (Shell No. 1, R/h = 100).
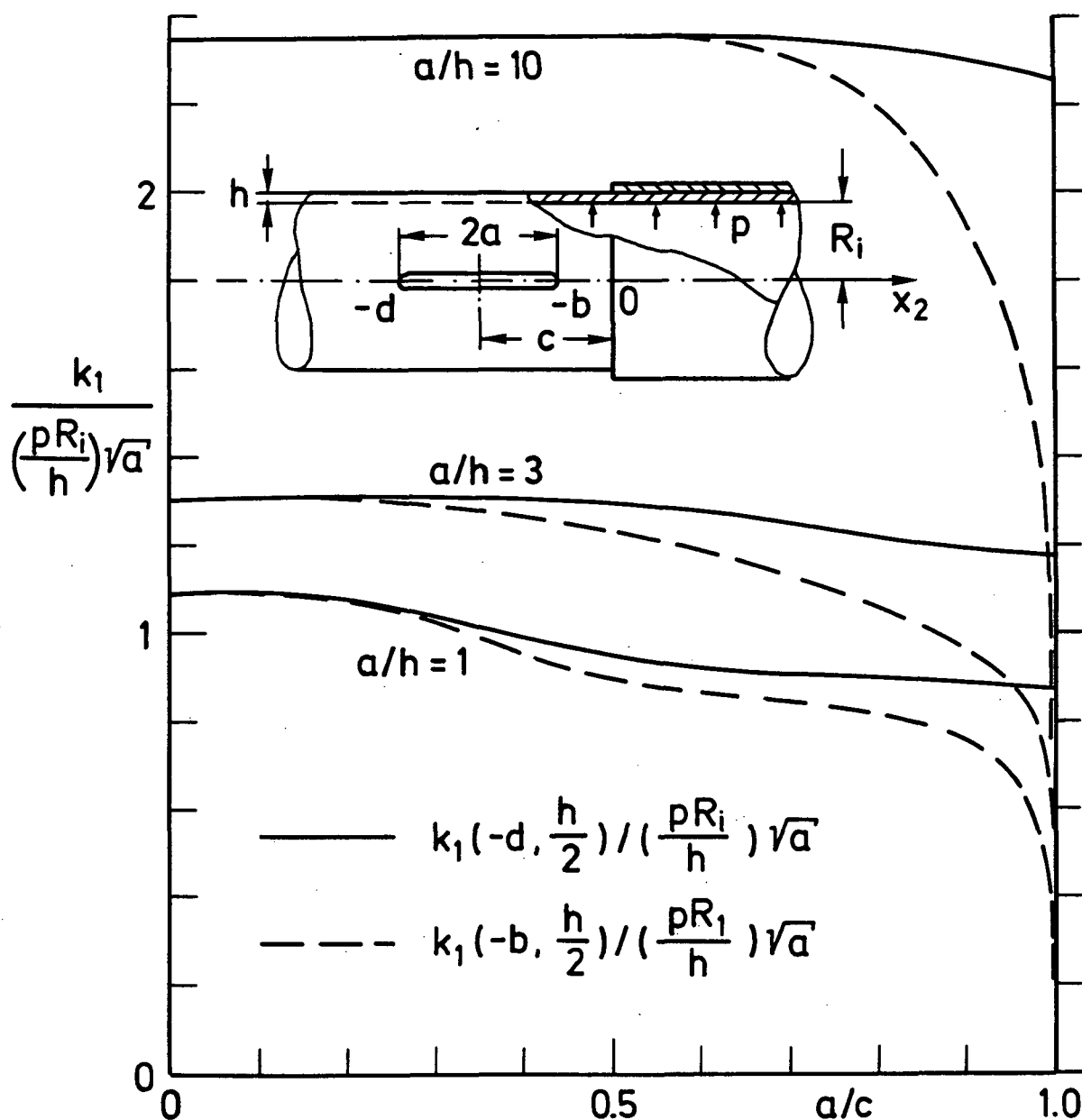
Fig. 3   Normalized stress intensity factors on the outside surface of an "open-ended" reinforced cylindrical shell containing an axial through crack (Shell No. 3, R/h = 35.5).
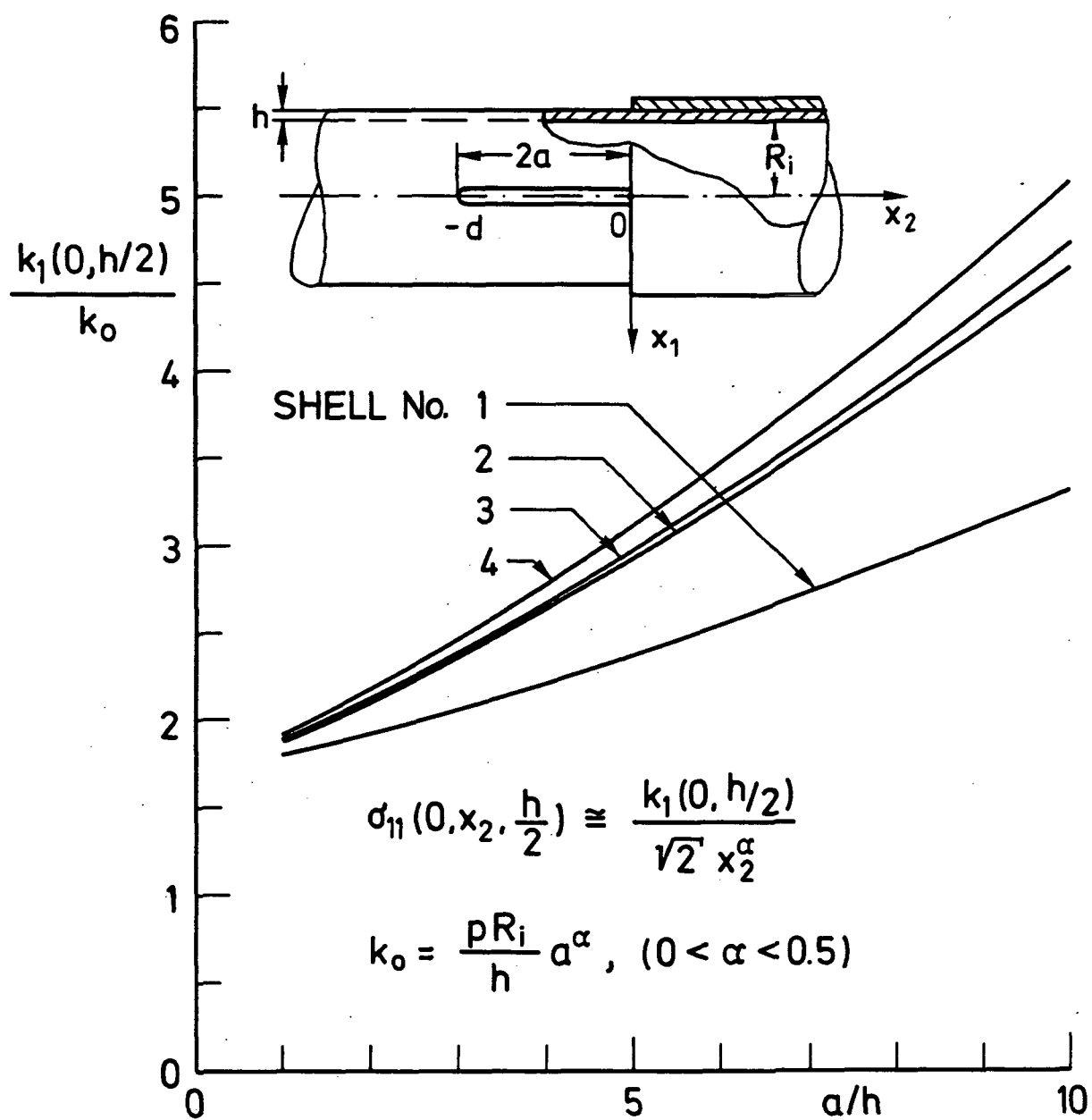
$$\sigma_{11}\left(0, x_2, \frac{h}{2}\right) \cong \frac{k_1\left(0, h/2\right)}{\sqrt{2}\, x_2^\alpha}$$

$$k_0 = \frac{pR_i}{h} a^\alpha, \quad (0 < \alpha < 0.5)$$

Fig. 4   Normalized stress intensity factor at the crack tip $x_2=0$ on the outside surface $x_3=h/2$ in "open-ended" reinforced cylindrical shells (see Table 1 for the dimensions of the shells and for the values of $\alpha=-\gamma$ for each shell).
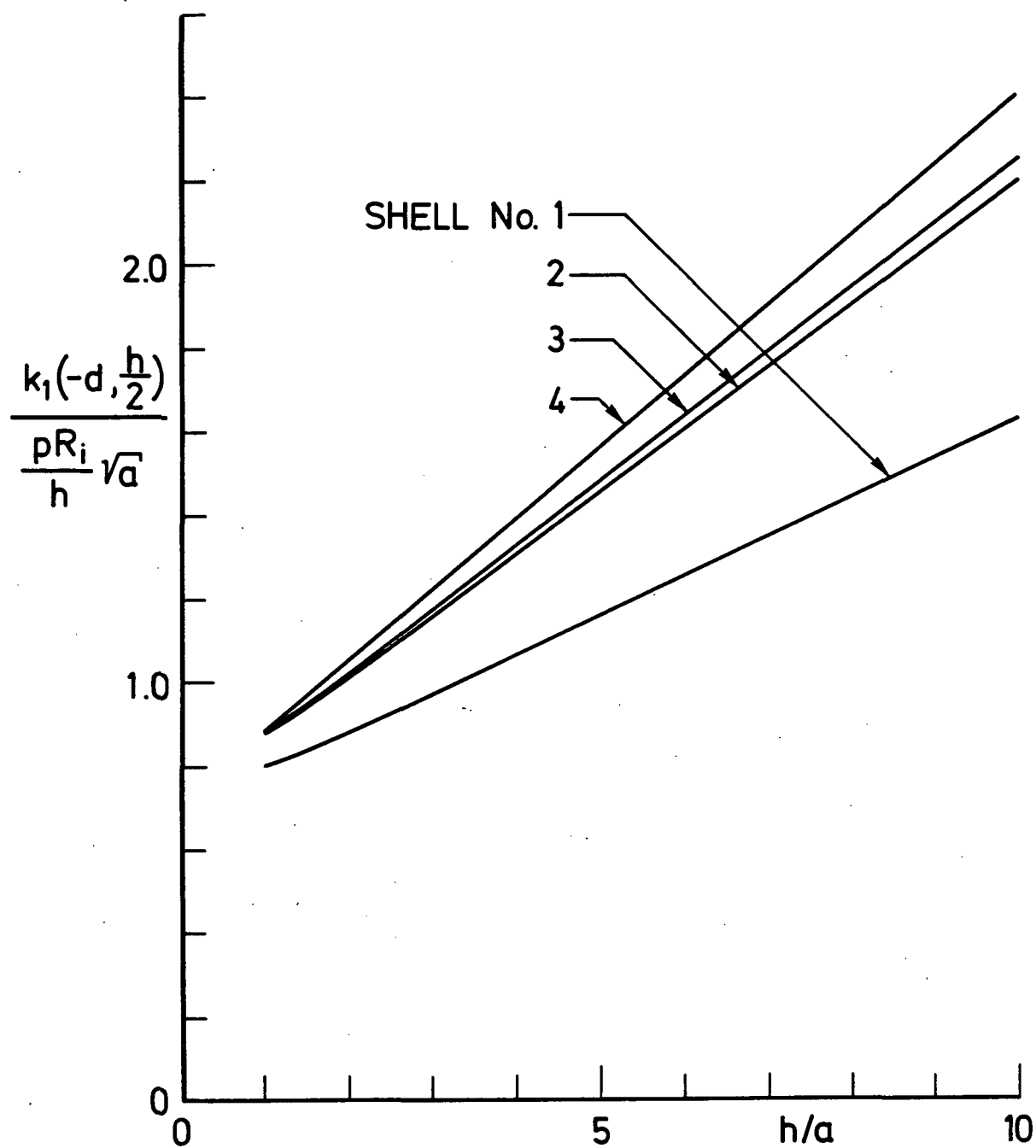
Fig. 5   Normalized stress intensity factor at the far end $x_2 = -d$ of a through crack intersecting the interface in "open-ended" reinforced cylindrical shells (see insert in Fig. 4 for geometry and Table 1 for dimensions of the shells).